Spectroscopy 18 (2004) 311–322
IOS Press

RAG1 oligomerization states and secondary structural properties: an initial characterization of V(D)J recombinase complex formation

LeAnn J. Godderz and Karla K. Rodgers *
Department of Biochemistry and Molecular Biology, University of Oklahoma Health Sciences Center, 940 Stanton L. Young Blvd, Oklahoma City, OK 73104, USA

Abstract. The recombination activating gene products (RAG1 and 2) catalyze the initial DNA cleavage steps during V(D)J recombination for the diversification of the immune repertoire. As the fundamental properties of the RAG proteins remain largely unknown, our objective is to investigate the self-association and conformational properties of RAG1. To analyze RAG1 association and dissociation, a time course of multi-angle laser light scattering measurements (MALL SEC) was performed on samples at different oligomerization states over a wide range of ionic strengths. The molecular masses of the predominant RAG1 species corresponded to dimer, tetramer, and a previously uncharacterized octamer state. Furthermore, the fraction of RAG1 in the tetrameric and octameric states increased significantly over time at lower ionic strengths, indicating that these oligomeric forms may factor into the physiological function of RAG1. Circular dichroism (CD) analysis of RAG1 showed a significant dependence in secondary structure on ionic strength with changes in α-helical content over time that may correspond to the changes in oligomerization states shown by MALLS SEC. Together, the MALLS SEC and CD analyses of RAG1 self-association properties and secondary structure give further insight into formation of the protein complex responsible for catalyzing V(D)J recombination.

1. Introduction

V(D)J recombination is responsible for assembling the immunoglobulin and T cell receptors in developing lymphocytes [11,13,19]. In this process, gene segments from two or three different pools termed V (variable), D (diversity), and J (joining) are selected and joined together to form functional genes containing the sequence diversity necessary for antigen specific receptors. Two lymphoid-specific proteins, RAG1 and RAG2 (recombination activating gene products 1 and 2), form the VDJ recombinase that catalyzes the initial DNA cleavage step in the recombination reaction [23]. Recombination signal sequences (RSS) flank each V, D, and J segment and direct the RAG proteins to the cleavage sites [19]. The RSS consists of conserved heptamer and nonamer sequences separated by a spacer of 12 or 23 base pairs. Efficient V(D)J recombination occurs only between RSS of dissimilar spacer lengths, a stipulation known as the 12/23 rule.

The mechanism of V(D)J recombination occurs in two phases. In phase 1, the recombinase binds to the DNA at the RSS and induces a single stand nick at the border between the RSS and the V, D, or

*Corresponding author. Tel.: +1 405 271 2227; Fax: +1 405 271 3139; E-mail: karla-rodgers@ouhsc.edu.

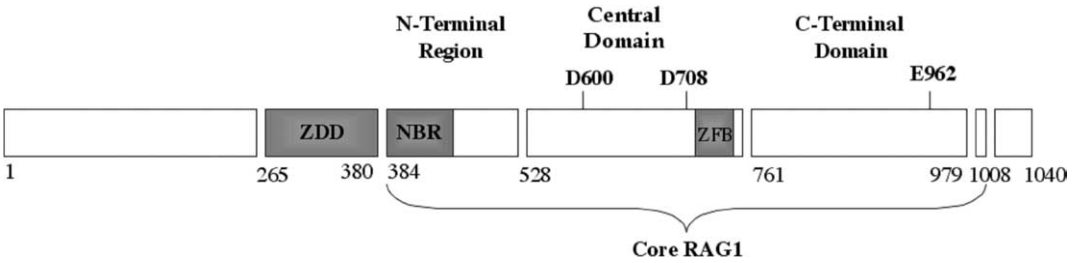

Fig. 1. Schematic diagram of RAG1 domains and active site. Full length RAG1, depicted here, consists of 1040 residues. The core region (384–1008) includes the N-terminal region (384–527), central domain (528–760), and C-terminal domain (761–979). Located within the core region, the DDE triad comprises the active site of RAG1 and contains residues D600, D708, and E962. *ZDD*, zinc dimerization domain; *NBR*, RSS nonamer-binding region; *ZFB*, zinc finger motif.

J coding segment. The resulting 3′ hydroxyl group of the coding segment then performs nucleophilic attack on the opposite strand of the DNA, resulting in a covalently sealed hairpin structure in the DNA at the terminal end of the coding segment and a double stranded break between the RSS and coding segment [23]. After the DNA is cleaved in the first step, the RAG proteins remain bound to both the signal [1] and the coding ends [16], perhaps directing the joining process in phase 2, where the ends of the two coding segments (coding ends) are processed and joined together and the ends of the two RSSs (signal ends) are joined by proteins in the non-homologous end joining pathway of DNA repair [13,21].

The majority of studies on the RAG proteins have used the core regions of both proteins. Expressed as a fusion to maltose binding protein (MBP), the core region of RAG1 is soluble and contains all the DNA binding properties and the active site necessary for full activity as compared to the full-length protein [13]. Shown in Fig. 1, the core region of RAG1 consists of residues 384–1008 of 1040 [31, 33]. A triad of acidic residues (Asp600, Asp708, and Glu962) called the DDE motif is located within core RAG1 [12,17,18]. This motif is necessary for RAG endonucleolytic activity. It is speculated to coordinate one or two divalent metal cations as do other enzymes with the motif [15]. Core RAG1 binds to the canonical RSS with specificity for both the nonamer and the heptamer regions [2,29].

Several regions within RAG1 important for its function during V(D)J recombination have been identified. The N-terminal region of core RAG1 contains the nonamer binding region (NBR). This region spans residues 384–454 (see Fig. 1) and recognizes the nonamer of the RSS [9,35]. The central domain (528–760) within core RAG1 binds specifically to the RSS heptamer [4] with strong affinity when the DNA is in single stranded form, indicating a conformational change in the RSS at the heptamer during the mechanism of V(D)J recombination [25]. RAG2 does not appear to bind the DNA directly, but rather to facilitate interaction between RAG1 and the RSS, possibly by inducing a conformational change within RAG1 or the RSS [10,14,38].

Multiple protein–DNA complexes participate during V(D)J recombination. Specifically, during phase 1, the RAG proteins can bind to a single 12 or 23 RSS independently (a single RSS complex) or to both simultaneously (a paired complex) [16]. Under physiological conditions, the nick can occur in either complex, but formation of the hairpin requires the paired complex [40]. The single and paired complexes of phase 1 are still largely undefined, with conflicting reports on the stoichiometry of RAG1 and RAG2 in each complex [5,24,37,38].

Understanding both the homo- and hetero-oligomerization properties of the RAG proteins is essential in elucidating the macromolecular interactions of the reaction, since multiple complexes may play roles in both phase 1 and phase 2. It was previously shown that RAG1 forms dimeric [29] and tetrameric species [14] in solution able to complex with RAG2 and bind to DNA [14]. The structural and oligomer-

ization properties of RAG1 have been reported to be sensitive to salt concentration, indicating that ionic interactions are involved [14]. Here we examined the association and dissociation of separated RAG1 oligomers, as well as changes in secondary structure, at different ionic strengths over time. We discovered an octameric form of RAG1 stabilized at lower ionic strengths similarly to the tetramer. In addition, dimer and octamer demonstrate a difference in secondary structure with structural changes over time and in response to ionic strength that correspond to subunit association and dissociation.

2. Results

2.1. Oligomeric species of core RAG1

Multi-angle laser light scattering (MALLS) analysis gives the absolute mass of macromolecules independent of molecular shape. Individual species can be analyzed separately when size exclusion chromatography (SEC) is coupled with MALLS, allowing separation of components into fractions [39]. SEC data used alone for mass measurements by comparison of elution profiles of proteins with known molecular masses is subject to misinterpretation due to shape dependent factors contributing to the elution profile. Previous studies using SEC indicated that core RAG1 fused to MBP (MCR1) is predominantly dimeric in solution [29]. However, studies using MALLS SEC resolved a second major species, tetramer MCR1, that also exists in solution [14]. Furthermore, the presence of additional higher order species was predicted, although the results were inconclusive. For further analysis of the association and dissociation properties of core RAG1 oligomers, we pooled two separate species of RAG1 after the gel filtration step of purification in buffer containing 0.2 M NaCl for use in MALLS SEC and circular dichroism (CD) studies: sample that eluted as predominantly dimer with some tetramer (referred to as the dimer:tetramer sample) from gel filtration during purification and sample that eluted earlier as higher order oligomer. Representative molecular mass distribution plots are shown in Fig. 2, panels A and B, for the dimer:tetramer and the higher order oligomer samples, respectively. In panel A, two separate peaks eluted from a Superdex 200 column were detected by light scattering. Peak 2 represents the predominant species as it is the most intense peak. Its calculated molecular mass of 254.5 ± 0.7 kDa is within 10% of the predicted molecular mass of 231 kDa for dimeric MCR1 based on amino acid composition. The plateau in the molecular mass profile at peak 2 indicates that the species is monodisperse across the peak.

Peak 1 yields an average molecular mass of 465.7 ± 3.0 kDa which corresponds well to the predicted molecular mass for tetrameric MCR1 (462 kDa). The incline in the molecular mass profile at peak 1 indicates that the species is somewhat polydisperse. A small percentage of oligomers of a higher order than tetramer are likely unresolved from the tetramer by the Superdex 200 column. That the molecular mass is within 1% of the predicted molecular mass for tetrameric MCR1 indicates that the concentration of the oligomers of higher order than tetramer is small in the sample, with their larger size giving a disproportionably greater contribution to the light scattering signal.

Importantly, no plateaus in the molecular mass profile or peaks in the elution profile are present for monomeric or trimeric MCR1, consistent with earlier studies [14]. Furthermore, the oligomerization of MCR1 is due solely to the core region, rather than to the MBP tag. The elution profile of MBP shows a single monodisperse peak [14], consistent with small-angle X-ray scattering measurements demonstrating that MBP is monomeric up to concentrations of 20 mg/ml [27]. Last, although the non-core regions of RAG1 may contribute to the oligomerization properties of full length RAG1 by extending the oligomerization interfaces, they likely do not affect the types of species formed. The ZDD domain

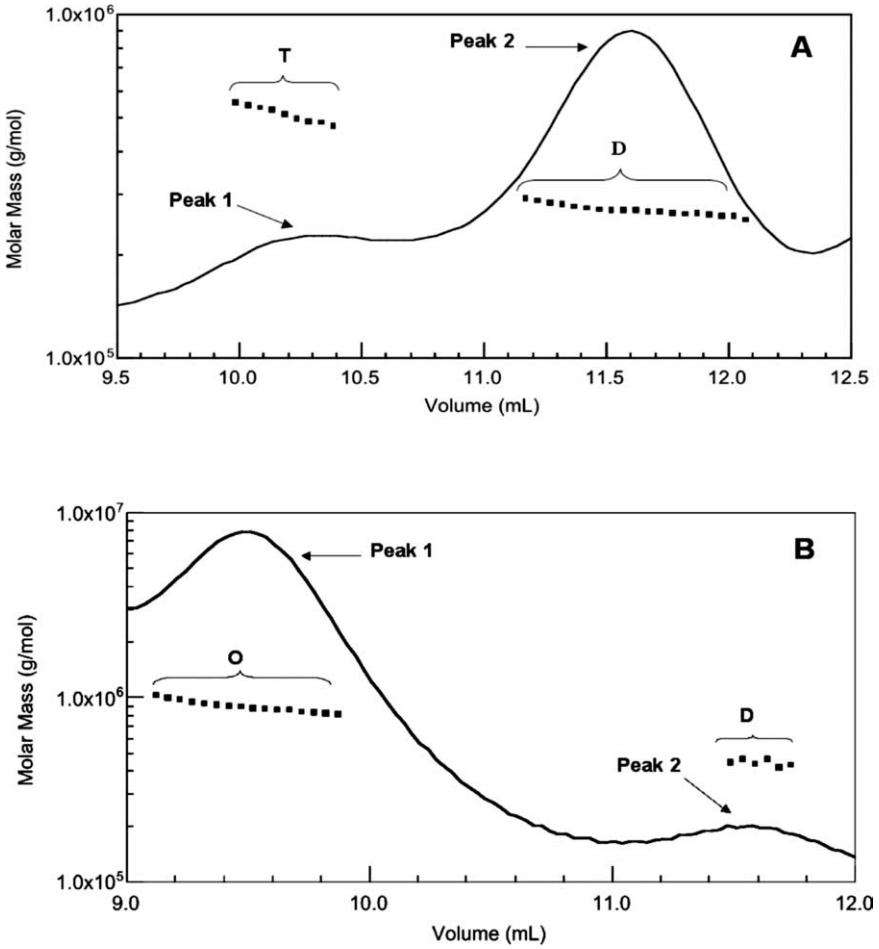

Fig. 2. Analysis of MBP-core RAG1 oligomerization states. Molar mass distribution plots representing the results obtained by subjecting MBP-core RAG1 dimer:tetramer (A) and higher order oligomer (B) samples to MALLS-SEC are shown. The continuous solid line represents the elution profile of MBP-core RAG1 from a Superdex 200 column as monitored by a refractometer detector. The molecular mass profile measured by light scattering (filled squares, plotted versus left axis) of the material that eluted at the corresponding volumes is overlaid on the elution profile. The bracketed plateaus labeled D, T, and O represent sample that eluted at molecular masses corresponding to dimeric, tetrameric, and octameric forms of MBP-core RAG1, respectively. The chromatographic buffer in this experiment included 0.2 M NaCl.

(residues 265–380) expressed by itself as a fusion to MBP forms a dimer at micromolar concentrations [27]. Previous MALLS SEC studies of MBP-RAG1zc (residues 265–1008 fused to MBP) show no altered oligomerization states, although the ratio of tetramer to dimer is enhanced [14].

To further investigate the higher order oligomeric forms of MCR1, we performed MALLS SEC analysis on sample pooled early in the elution profile during purification to determine whether there are stable oligomers higher than tetramer that can dissociate to dimer. The molar mass distribution plot is shown in panel B (Fig. 2). Peak 1, the predominant species in this sample, demonstrates a molecular mass of 902.5 ± 0.040 kDa which is within 2.3% of the predicted molecular mass for octameric MCR1 (924 kDa). In the higher order oligomer sample, peak 1 is shifted about 0.7 ml earlier in the elution profile, as compared to peak 1 in the dimer sample in panel A. This is consistent with peak 1 in panel B being octamer

as compared to the tetrameric species in panel A. In panel B, peak 2 corresponds to dimeric MCR1. It is a very minor species, constituting only 10% of the total sample by peak integration.

Interestingly, no tetramer intermediate is detected in the octamer sample. There are several possibilities to explain its absence. It is possible that the octamer may directly dissociate into dimer. A second possibility is that the tetramer and octamer may be in fast exchange in peak 1, with the major form in the peak reflected by the molecular mass. Last, both octamer and tetramer may exist in stable forms yet be difficult to resolve due to limitations of the column at such high molecular weights. If low quantities of the tetramer are present, their presence could be masked by the higher molecular weight of the octamer. In any case, the octameric form is the major species of RAG1 in the higher oligomeric sample.

2.2. *Ionic strength dependence of core RAG1 oligomerization versus time*

ASV and HIV integrase both contain a DDE motif, similar to RAG1. Since distribution into multiple oligomers for ASV and HIV varies with solution conditions [6,8] it was speculated that RAG1 may also exhibit changes in oligomerization based on ionic strength or changes in pH. Although it was shown that no significant change in RAG1 oligomerization occurs with change in pH, it was found that decreasing ionic strength leads to an increase in higher order oligomeric forms [14]. To examine the relationship between ionic strength and oligomerization of different RAG1 species, we performed experiments at three different ionic strengths with each solution condition monitored versus time. The percent of each oligomeric species was determined by peak integration of the MALLS SEC data. Figure 3A shows results from the time course studies on dimeric MCR1, in which the light scattering buffer contained 0.2 M NaCl. Over time, at 0.2 M NaCl, MCR1 dimer increasingly associates to tetramer. From 0 to 48 hours, the dimeric content decreases from 69.2% to 63.9% (Fig. 3B) as tetrameric content correspondingly increases from 30.8% to 36.1%. While the MCR1 purification was done in 0.2 M NaCl, the initial fractionation to obtain the dimer:tetramer sample likely did not include all the tetrameric species. Thus we observe reassociation of dimer to tetramer to reestablish equilibria. However, it is apparent from Fig. 3B that achieving equilibrium occurs over a relatively long time period of days. Figure 3B also shows the percent of dimer in the dimer:tetramer MCR1 sample over a period of 48 hours at 0.5 and 1.0 M NaCl concentrations. This figure shows an increased dissociation to dimeric species over time at buffer conditions of 0.5 M and 1 M NaCl. From 0 to 48 hours, the dimer content increases from 79.6% to 86.7% and from 82.8% to 89.7% for 0.5 M and 1 M NaCl samples, respectively. Between 24 and 48 hours, the curves begin to level off as samples approach equilibrium. This is in contrast to the previous results at 0.2 M NaCl, in which, as described above, dimeric MCR1 associates to tetramer.

By 48 hours, the changes in oligomerization have neared equilibrium to enable an estimate of the association constant (K_a). Since the changes are slow, occurring over a time frame of several days, a reasonable estimate of the equilibrium constant from gel filtration data can be obtained [22]. The K_a values determined below could be somewhat underestimated due to the small degree of dilution that may occur on the gel filtration column. However, this is likely not a major factor, given the apparent slow exchange of subunits. The assembly from dimer to tetramer may be described by the following equation:

$$2D \rightleftarrows T \tag{1}$$

with the association constant as follows:

$$K_a = T/D^2, \tag{2}$$

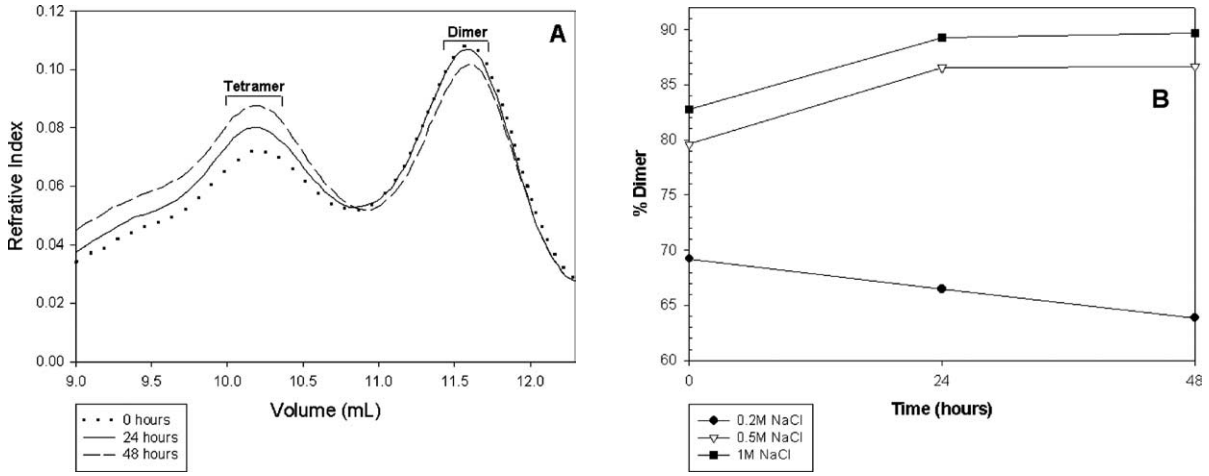

Fig. 3. Analysis of MBP-core RAG1 dimer:tetramer oligomerization. (A) The molar mass distribution plot for MALLS-SEC analysis performed on dimer:tetramer MBP-core RAG1 at 0 hours (·····), 24 hours (——), and 48 hours (- - - - -) is shown. Brackets indicate sample that eluted from the column at the molecular weights corresponding to dimeric and tetrameric MBP-core RAG1. (B) The percent dimer composition of MBP-core RAG1 dimer sample versus time is shown at 0.2 M NaCl (circles), 0.5 M NaCl (triangles), and 1.0 M NaCl (squares). Percent dimer is calculated by peak integration of the dimer and tetramer peaks from the MALLS-SEC data.

where $T = (D_{\mathrm{T}} - D)/2$, $D_{\mathrm{T}} =$ the concentration of protein loaded onto the column, and $D =$ the fraction of protein in the dimer peak $\times D_{\mathrm{T}}$. Using these equations and the MALLS SEC data at 48 hours, the K_{a} for RAG1 dimer association to tetramer is estimated to be approximately 8.21×10^4 M^{-1} at 0.2 M NaCl, 1.77×10^4 M^{-1} at 0.5 M NaCl, and 1.42×10^4 M^{-1} at 1.0 M NaCl. The higher K_{a} at 0.2 M NaCl corresponds to the higher association to tetramer at that salt. In addition, these values predict dimeric RAG1 to be the major species present at μM levels of RAG1 as shown by MALLS SEC analysis.

Figure 4A shows the MALLS SEC time course performed on octameric MCR1 at 0.5 M NaCl. From 0 to 48 hours, the octameric content slowly dissociates from 84.1% to 76.1% as dimeric content correspondingly increases from 15.9% to 23.9%. The percentages of octameric species present over time for all three ionic strengths are shown in Fig. 4B. At 0.5 M and 1 M NaCl, octameric MCR1 slowly dissociates to dimeric species. The octamer state appears to have a considerably slower off rate than tetramer. At the time points tested, the octamer to dimer dissociation is not yet approaching equilibrium, so no K_{a} values are reported here. Octameric content decreases from 84.1% to 76.1% and from 81.7% to 74.1% at 0.5 M and 1 M NaCl, respectively. In contrast, at 0.2 M NaCl, octamer is fairly stabilized with a minimal decrease of 1.2%. These results indicate that at near physiological ionic strengths (0.2 M NaCl) the higher order oligomeric forms of RAG1 are significantly stabilized by electrostatic interactions.

2.3. Secondary structural analysis of core RAG1

In addition to the self-association properties of core RAG1, we have also investigated the secondary structure of RAG1 in different ionic strengths over time. CD spectroscopy was used to analyze the secondary structure of core RAG1. Three programs CONTIN, SELCON3, and CDSSTR were used for the analysis – a combination which gives a higher accuracy, even with a reduced spectral range ($\lambda \approx 200$–300 nm) [26,36]. We focused on α-helical structure since it yields the most significant change and is

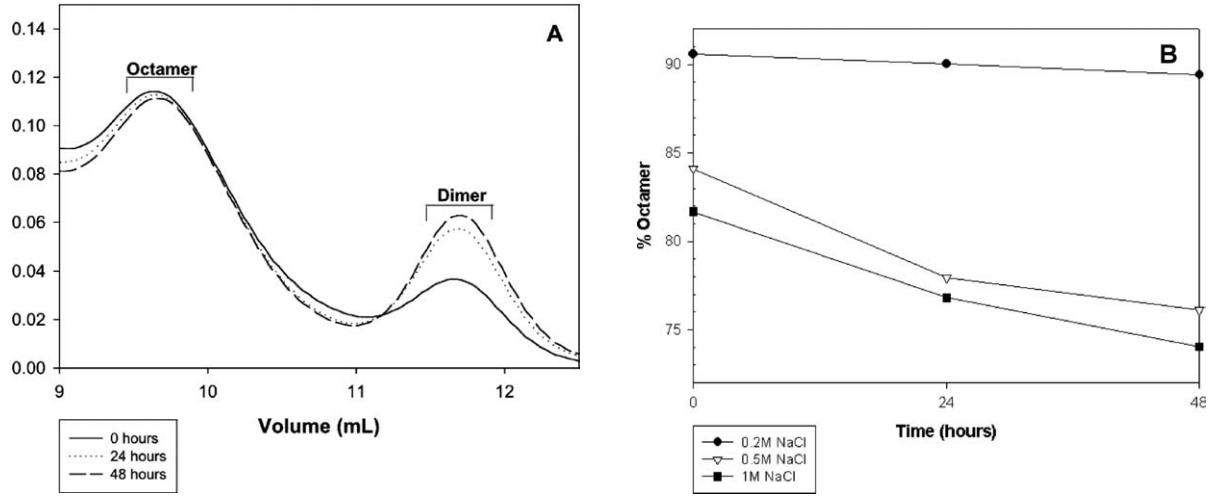

Fig. 4. Analysis of MBP-core RAG1 octamer oligomerization. (A) The molar mass distribution plot for MALLS-SEC analysis performed on octameric MBP-core RAG1 at 0 hours (· · · · ·), 24 hours (——), and 48 hours (- - - - -) hours at 0.2 M NaCl is shown. Brackets indicate sample that eluted from the column at the molecular weights corresponding to dimeric and octameric MBP-core RAG1. (B) The percent higher order oligomer composition of MBP-core RAG1 octamer sample versus time is shown at 0.2 M NaCl (circles), 0.5 M NaCl (triangles), and 1.0 M NaCl (squares). Percent octamer is calculated by peak integration of the dimer and octamer peaks from the MALLS-SEC data.

the most accurately determined secondary structural element within this wavelength range [36]. Previous measurements of RAG1 secondary structure used a mixture of dimer and higher order oligomers. These studies showed an increase in α-helical content with increasing ionic strength [14]. In this study, core RAG1 was separated into dimer:tetramer and octamer samples to investigate structural differences between the oligomeric states in addition to changes in response to ionic strength over time during the association and dissociation processes. Shown in Fig. 5A are the CD spectra for dimer:tetramer and octamer core RAG1 at 0.2 M NaCl measured immediately after purification. The dimer:tetramer sample has 18.6% more α-helical structure than the octamer sample. The results from the CD time course at different ionic strengths are shown in Fig. 5B. Both dimer:tetramer and octamer samples lost α-helical structure from 0 to 48 hours, but the % decrease in α-helix was greatest (from 51.2% to 32.1%) at 0.2 M NaCl for the dimer:tetramer sample. This could be due to the loss of dimer over time, corresponding with the results from the MALLS SEC studies, where at 0.5 M NaCl and 1.0 M NaCl, over time, dimer increases while tetramer and octamer decrease, but at 0.2 M NaCl, dimer associates to tetramer and the octamer species is stabilized. In addition, each day, from 0.2 M NaCl to 1 M NaCl, the α-helical content increased for dimer:tetramer sample, but decreased for octamer sample. At higher salt concentrations, the increase of dimer in the dimer:tetramer sample could result in the increase in α-helical content. Since the octamer has a slower off rate, it is possible that the loss of octamer structure at the higher salt concentrations was not completely compensated by the slow increase in dimer structure.

2.4. Free energy of core RAG1 association

Using the data from the previous sections, an estimate of the free energy of RAG1 association and an overall model may be formulated. From the K_a values determined from the MALLS SEC data, ΔG values are -6.23, -5.38, and -5.26 kcal/mol for 0.2 M, 0.5 M, and 1.0 M NaCl, respectively.

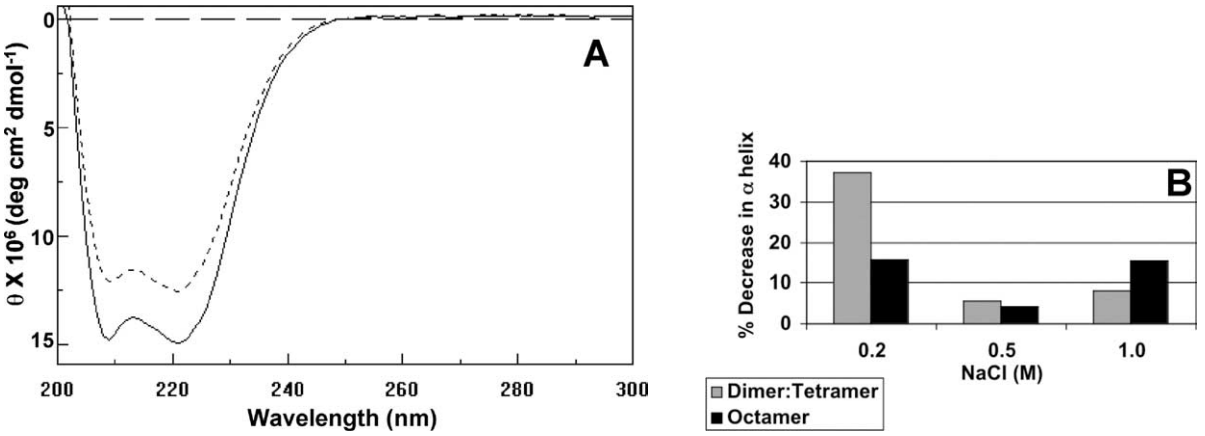

Fig. 5. CD spectroscopy of MBP-core RAG1. (A) The CD spectra for dimer:tetramer MCR1 (——) and octameric MCR1 (- - - - -) at 0.2 M NaCl are shown. CD spectra are in units of molar ellipticity versus wavelength. (B) The bar graph depicts the % decrease from initial time point to 48 hours in MBP-core RAG1 α-helical structure versus salt concentration as determined by CD structural analysis. Analysis was performed on dimer:tetramer MBP-core RAG1 (gray bars) and octamer MBP-core RAG1 (black bars).

Salt dependent changes in equilibrium constants indicate that ions are involved in the association process. Assuming that hydration interactions are small,

$$\delta \ln K_{\mathrm{a}}/\delta \ln[\mathrm{NaCl}] \approx -\Delta v_{\mathrm{Na+Cl}} \tag{3}$$

where $\Delta v_{\mathrm{Na+Cl}} =$ the number of mole equivalents of ions released during association [7]. By this equation, the number of charged groups involved in stabilizing the tetramer may be estimated. At the change from 0.5 M to 0.2 M NaCl, $\delta \ln K_{\mathrm{a}}/\delta \ln[\mathrm{NaCl}] = -1.7$, indicating the release of approximately 2 ions during the association reaction. The ion release is much smaller from 1.0 M to 0.5 M: 0.3 ion mole equivalents. The change in the $\delta \ln K_{\mathrm{a}}/\delta \ln[\mathrm{NaCl}]$ value from 0.2 to 0.5 M NaCl and 0.5 to 1.0 M NaCl indicates that ionic interactions change with increasing [NaCl] but does not reveal whether conformational changes or surface interactions, such as salt bridges, between the associating molecules are responsible. Depending on the nature of the surrounding environment, a single salt bridge may contribute from 0.5 kcal/mol [28,32] to 3 kcal/mol [3] of free energy. The $\Delta\Delta G$ from 0.2 to 1.0 M NaCl is approximately 1.0 kcal/mol; therefore, the increase in tetramer formation at 0.2 M NaCl versus 1.0 M NaCl is due to the formation of, at most, two salt bridges. We speculate that the free energy for tetramer stability changes with ionic strength and can be represented by the diagram in Fig. 6.

3. Discussion

To understand the mechanism of V(D)J recombination, it is important to systematically study the macromolecular interactions occurring at each step in the reaction. We have begun our investigation with RAG1 as it contains the DNA binding motifs and the active site necessary for activity of the recombinase [4,9,35]. Here we report self-association properties and secondary structural traits of separate dimer and octamer samples of core RAG1. Previous MALLS SEC studies have identified dimeric and tetrameric states of RAG1 [14]. Here we have identified a stable octamer species able to dissociate into dimer. Although tetramer and dimer are probably the major forms of core RAG1, the octamer (most stable at

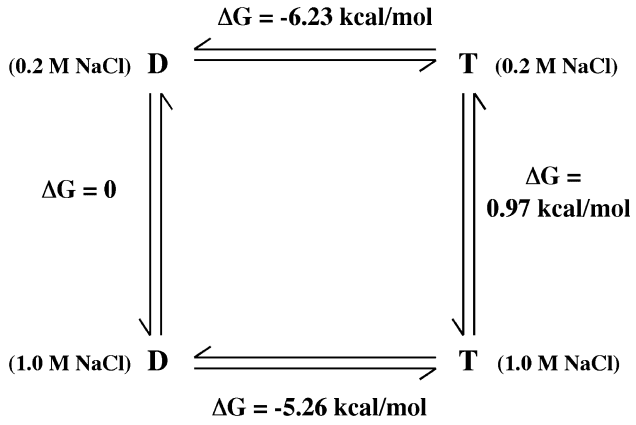

Fig. 6. Free energy model of RAG1 dimer:tetramer oligomerization. A model for dimer to tetramer oligomerization is shown. ΔG values are calculated as described in text for dimer to tetramer transitions. A ΔG value of zero is assumed for the transition from dimer at 0.2 M NaCl to dimer at 1.0 M NaCl. The ΔG value for the transition from tetramer at 0.2 M NaCl to tetramer at 1.0 M NaCl is calculated using the measured ΔG values for the dimer:tetramer equilibria (see text). D, dimer MCR1; T, tetramer MCR1.

physiological ionic strength) may serve some function during V(D)J recombination, such as a negative regulatory role as a reservoir of RAG1. RAG2 is regulated during the cell cycle [20] while RAG1 is typically long-lived [30] and perhaps regulated by other means.

The estimated association of RAG1 to the higher order oligomers is relatively weak. According to the estimated K_a, RAG1 exists mostly as dimer at μM concentrations, but the higher oligomeric forms are not in fast exchange with the dimer and demonstrate appreciably slow off rates. In addition, the physiological concentration of RAG1 is not known; within the nucleus, immunofluorescence studies have shown that RAG1 and RAG2 are enriched within discrete regions [34] (William Rodgers, personal communication). This would significantly increase local protein concentration, possibly inducing the formation of the higher order oligomers, which once they form are extremely stable. Furthermore, RAG2 or the specific RSS sequence may affect the equilibrium *in vivo*, stabilizing a particular oligomeric state. Of note, SEC studies have indicated that the presence of the RSS induces tetramer formation [14]. Significantly, at ionic strength close to physiological levels (0.2 M NaCl), the higher order oligomers are most stable and association from dimer to tetramer is most favored. If a conformational change is induced at the lower ionic strengths, as suggested by the CD analysis, this could be responsible for the slow off rate. Together, these results suggest that electrostatic interactions at low salt concentrations (0.2 M) prefer the tetrameric state and may be responsible for inducing certain conformational changes important during V(D)J recombination.

4. Experimental

MBP fused to core RAG1, referred to as MBP-core RAG1 (MCR1), is encoded by plasmid pCJM233 as previously described [29]. MCR1 was expressed in *Escherichia coli* and purified as previously described with the following exceptions [4]. The MALLS SEC buffer and CD buffer described below (containing 0.2 M NaCl) were used as the gel filtration buffer for purifying the MCR1 that was used in the respective experiments.

MALLS SEC was performed using a DAWN DSP laserphotometer coupled with an Optilab DSP interferometric refractometer (Wyatt Technology, Santa Barbara, CA) and combined in-line with a Superdex 200 HR 10/30 gel filtration column (Amersham Pharmacia, Piscataway, NJ). The column buffer was comprised of 20 mM Tris pH 8.0, 50 μM $ZnCl_2$, 5 mM β-mercaptoethanol (BME), and 0.2, 0.5, or 1.0 M NaCl. Protein was pooled into dimer or higher order oligomer samples immediately from the HPLC step of purification, concentrated, and adjusted to the proper salt concentration prior to MALLS SEC measurements. During the time course, protein was stored at 4°C between measurements to stabilize the protein. For each experiment, initial protein concentrations were between 1.1 and 1.6 mg/ml. Astra 4.72 software was used to perform the molecular mass calculations. On the basis that the refractive input is considered constant from unmodified proteins, the dn/dc values were set at 0.19 for the molecular mass calculations [39].

The CD spectroscopy experiments were accomplished using a JASCO J715 Spectropolarimeter with a PTC-348WI peltier temperature controller (Jasco, Corp., Tokyo, Japan). Spectral parameters were as follows: 300–200 nm wavelength range, 0.1 cm cuvette pathlength, and 10 accumulations per spectrum. All CD measurements were performed at 20°C. CD buffer consisted of 10 mM Tris pH 8.0, 10 μM $ZnCl_2$, 1 mM BME, and 0.2, 0.5, or 1.0 M NaCl. Use of BME was needed for preventing protein crosslinking and disruption of zinc binding sites [27]. Protein was pooled into dimer or higher-order oligomer samples immediately from the gel filtration step of purification and adjusted to the proper salt concentration prior to CD measurements. During the time course, protein was stored at 4°C between measurements. Final protein concentrations were between 0.11 and 0.23 mg/ml. The CDPro software package (available online at http://lamar.colostate.edu/∼sreeram/CDPro) was used to obtain protein secondary structural content [36]. The three programs offered in the software package, CONTIN, SELCON3, and CDSSTR, were run using the same 43 protein reference library. For each protein sample, the values obtained from the software calculations were averaged to give the α-helix and β-sheet percentages.

Acknowledgements

We thank Bruce Baggenstoss for valuable technical assistance. This work was supported by Research Project Grant RPG-00-032-01-CIM from the American Cancer Society, an Oklahoma Center for Advancement in Science and Technology award for project number HR02-008, and National Institutes of Health grant RR15577. L.J.G. is supported by a National Science Foundation Graduate Research Fellowship.

References

[1] A. Agrawal and D.G. Schatz, RAG1 and RAG2 form a stable postcleavage synaptic complex with DNA containing signal ends in V(D)J recombination, *Cell* **89** (1997), 43–53.
[2] Y. Akamatsu and M.A. Oettinger, Distinct roles of RAG1 and RAG2 in binding the V(D)J recombination signal sequences, *Mol. Cell. Biol.* **18** (1998), 4670–4678.
[3] D.E. Anderson, W.J. Becktel and F.W. Dahlquist, pH-induced denaturation of proteins: a single salt bridge contributes 3–5 kcal/mol to the free energy of folding of T4 lysozyme, *Biochemistry* **29** (1990), 2403–2408.
[4] J.L. Arbuckle, L.J. Fauss, R. Simpson, L.M. Ptaszek and K.K. Rodgers, Identification of two topologically independent domains in RAG1 and their role in macromolecular interactions relevant to V(D)J recombination, *J. Biol. Chem.* **276** (2001), 37093–37101.
[5] T. Bailin, X. Mo and M.J. Sadofsky, A RAG1 and RAG2 tetramer complex is active in cleavage in V(D)J recombination, *Mol. Cell. Biol.* **19** (1999), 4664–4671.

[6] J. Coleman, S. Eaton, G. Merkel, A.M. Skalka and T. Laue, Characterization of the self-association of avian sarcoma virus integrase by analytical ultracentrifugation, *J. Biol. Chem.* **274** (1999), 32842–32846.
[7] M.A. Daugherty, M. Brenowitz and M.G. Fried, The TATA-binding protein from *Saccharomyces cervisiae* oligomerizes in solution at micromolar concentrations to form tetramers and octamers, *J. Mol. Biol.* **285** (1999), 1389–1399.
[8] E. Deprez, P. Tauc, H. Leh, J.F. Mouscadet, C. Auclair and J.C. Brochon, Oligomeric states of the HIV-1 integrase as measured by time-resolved fluorescence anisotropy, *Biochemistry* **39** (2000), 9275–9284.
[9] M.J. Difilippantonio, C.J. McMahan, Q.M. Eastman, E. Spanopoulou and D.G. Schatz, RAG1 mediates signal sequence recognition and recruitment of RAG2 in V(D)J recombination, *Cell* **87** (1996), 253–262.
[10] Q.M. Eastman, I.J. Villey and D.G. Schatz, Detection of RAG protein-V(D)J recombination signal interactions near the site of DNA cleavage by UV cross-linking, *Mol. Cell. Biol.* **19** (1999), 3788–3797.
[11] S.D. Fugmann, A.I. Lee, P.E. Shockett, I.J. Villey and D.G. Schatz, The RAG proteins and V(D)J recombination: complexes, ends, and transposition, *Annu. Rev. Immunol.* **18** (2000), 495–527.
[12] S.D. Fugmann, I.J. Villey, L.M. Ptaszek and D.G. Schatz, Identification of two catalytic residues in RAG1 that define a single active site within the RAG1/RAG2 protein complex, *Mol. Cell* **5** (2000), 97–107.
[13] M. Gellert, V(D)J recombination: RAG proteins, repair factors, and regulation, *Annu. Rev. Biochem.* **71** (2002), 101–132.
[14] L.J. Godderz, N.S. Rahman, G.M. Risinger, J.L. Arbuckle and K.K. Rodgers, Self-association and conformational properties of RAG1: Implications for formation of the V(D)J recombinase, *Nucleic Acids Res.* **31** (2003), 2014–2023.
[15] L. Haren, B. Ton-Hoang and M. Chandler, Integrating DNA: transposases and retroviral integrases, *Annu. Rev. Microbiol.* **53** (1999), 245–281.
[16] K. Hiom and M. Gellert, Assembly of a 12/23 paired signal complex: a critical control point in V(D)J recombination, *Mol. Cell* **1** (1998), 1011–1019.
[17] D.R. Kim, Y. Dai, C.L. Mundy, W. Yang and M.A. Oettinger, Mutations of acidic residues in RAG1 define the active site of the V(D)J recombinase, *Genes Dev.* **13** (1999), 3070–3080.
[18] M.A. Landree, J.A. Wibbenmeyer and D.B. Roth, Mutational analysis of RAG1 and RAG2 identifies three catalytic amino acids in RAG1 critical for both cleavage steps of V(D)J recombination, *Genes Dev.* **13** (1999), 3059–3069.
[19] S.M. Lewis, The mechanism of V(D)J joining: lessons from molecular, immunological and comparative analyses, *Adv. Immunol.* **56** (1994), 27–150.
[20] W.C. Lin and S. Desiderio, Cell cycle regulation of V(D)J recombination-activating protein RAG-2, *Proc. Natl. Acad. Sci. USA* **91** (1994), 2733–2737.
[21] Y. Ma, U. Pannicke, K. Schwarz and M.R. Lieber, Hairpin opening and overhang processing by an Artemis/DNA-dependent protein kinase complex in nonhomologous end joining and V(D)J recombination, *Cell* **108** (2002), 781–794.
[22] L.R. Manning, W.T. Jenkins, J.R. Hess, K.Vandegriff, R.M. Winslow and J.M. Manning, Subunit dissociations in natural and recombinant hemoglobins, *Prot. Sci.* **5** (1996), 775–781.
[23] J.F. McBlane, D.C. van Gent, D.A. Ramsden, C. Romeo, C.A. Cuomo, M. Gellert and M.A. Oettinger, Cleavage at a V(D)J recombination signal requires only RAG1 and RAG2 proteins and occurs in two steps, *Cell* **83** (1995), 387–395.
[24] C.L. Mundy, N. Patenge, A.G.W. Matthews and M.A. Oettinger, Assembly of the RAG1/RAG2 synaptic complex, *Mol. Cell. Biol.* **22** (2002), 69–77.
[25] M.M. Peak, J.L. Arbuckle and K.K. Rodgers, The central domain of core RAG1 preferentially recognizes single-stranded recombination signal sequence heptamer, *J. Biol. Chem.* **278** (2003), 18235–18240.
[26] J.T. Pelton and L.R. McLean, Spectroscopic methods for analysis of protein secondary structure, *Anal. Biochem.* **277** (2000), 167–176.
[27] K.K. Rodgers, Z. Bu, K.G. Fleming, D.G. Schatz, D.M. Engelman and J.E. Coleman, A zinc-binding domain involved in the dimerization of RAG1, *J. Mol. Biol.* **260** (1996), 70–84.
[28] K.K. Rodgers, T.C. Pochapsky and S.G. Sligar, Probing the mechanisms of macromolecular recognition: the cytochrome b5–cytochrome c complex, *Science* **240** (1988), 1657–1659.
[29] K.K. Rodgers, I.J. Villey, L. Ptaszek, E. Corbett, D.G. Schatz and J.E. Coleman, A dimer of the lymphoid protein RAG1 recognizes the recombination signal sequence and the complex stably incorporates the high mobility group protein HMG2, *Nucleic Acids Res.* **27** (1999), 2938–2946.
[30] A.E. Ross, M. Vuica and S. Desiderio, Overlapping signals for protein degradation and nuclear localization define a role for intrinsic RAG-2 nuclear uptake in dividing cells, *Mol. Cell. Biol.* **23** (2003), 5308–5319.
[31] M.J. Sadofsky, J.E. Hesse, J.F. McBlane and M. Gellert, Expression and V(D)J recombination activity of mutated RAG-1 proteins, *Nucleic Acids Res.* **21** (1993), 5644–5650.
[32] L. Serrano, A. Horovitz, B. Avron, M. Bycroft and A.R. Fersht, Estimating the contribution of engineered surface electrostatic interactions to protein stability by using double-mutant cycles, *Biochemistry* **29** (1990), 9343–9352.
[33] D.P. Silver, E. Spanopoulou, R.C. Mulligan and D. Baltimore, Dispensable sequence motifs in the *RAG-1* and *RAG-2* genes for plasmid V(D)J recombination, *Proc. Natl. Acad. Sci. USA* **90** (1993), 6100–6104.
[34] E. Spanopoulou, P. Cortes, C. Shih, C.M. Huang, D.P. Silver, P. Svec and D. Baltimore, Localization, interaction, and RNA binding properties of the V(D)J recombination-activating proteins RAG1 and RAG2, *Immunity* **3** (1995), 715–726.

[35] E. Spanopoulou, F. Zaitseva, F.-H. Wang, S. Santagata, D. Baltimore and G. Panayotou, The homeodomain region of Rag-1 reveals the parallel mechanisms of bacterial and V(D)J recombination, *Cell* **87** (1996), 263–276.
[36] N. Sreerama and R.W. Woody, Estimation of protein secondary structure from CD spectra: Comparison of CONTIN, SELCON, and CDSSTR methods with an expanded reference set, *Anal. Biochem.* **287** (2000), 252–260.
[37] P.C. Swanson, A RAG-1/RAG-2 tetramer supports 12/23-regulated synapsis, cleavage and transposition of V(D)J recombination signals, *Mol. Cell. Biol.* **22** (2002), 7790–7801.
[38] P.C. Swanson and S. Desiderio, RAG-2 promotes heptamer occupancy by RAG-1 in the assembly of a V(D)J initiation complex, *Mol. Cell. Biol.* **19** (1999), 3674–3683.
[39] J. Wen, T. Arakawa and J.S. Philo, Size-exclusion chromatography with on-line light-scattering, absorbance, and refractive index detectors for studying proteins and their interactions, *Anal. Biochem.* **240** (1996), 155–166.
[40] K. Yu and M.R. Lieber, The nicking step in V(D)J recombination is independent of synapsis: implications for the immune repertoire, *Mol. Cell. Biol.* **20** (2000), 7914–7921.